

Synthesis and characterization of pyrochlore-type yttrium titanate nanoparticles by modified sol–gel method

Z S CHEN^{1,2}, W P GONG^{1,3,*}, T F CHEN¹ and S L LI¹

¹State Key Laboratory of Powder Metallurgy, Central South University, Changsha, Hunan 410083, P.R. China

²Key Laboratory of Radioactive Geology and Exploration Technology Fundamental Science for National Defense, East China Institute of Technology, Fuzhou, Jiangxi 344000, P.R. China

³Electronic Science Department, Huizhou University, Huizhou, Guangdong 516001, P.R. China

MS received 29 August 2010; revised 21 October 2010

Abstract. Pyrochlore-type yttrium titanate ($Y_2Ti_2O_7$) nanoparticles were successfully synthesized by a simple soft-chemistry technique viz. citric acid sol–gel method (CAM). The preparation process was monitored by X-ray diffraction, thermogravimetric–differential thermal analysis and Fourier transform–infrared experiments and the microstructures and average size of as-prepared products were characterized by transmission electron microscopy and high resolution transmission electron microscopy images. It was found that compared with traditional solid state reaction (SSR), $Y_2Ti_2O_7$ nanopowders were synthesized at a relatively low temperature (750°C) for shortened reaction time. Detailed analysis showed that the as-prepared $Y_2Ti_2O_7$ with good dispersibility and narrow size distribution were quasi-spherical; the average size was about 20–30 nm, also, the obtained products had higher BET surface area (50 m²/g). These properties are very helpful for a photocatalyst to achieve excellent activity and may result in better behaviour in hydrogen storage.

Keywords. Yttrium titanate; sol–gel method; synthesis.

1. Introduction

Classical pyrochlore oxides, written using the general formula $A_2B_2O_7$ (where A is normally the larger trivalent cation and B the smaller quadrivalent one), exhibit space group $Fd\bar{3}m$ with eight formula units within the face-centred cubic unit cell (Subramanian *et al* 1983). Mostly, A is a trivalent rare-earth ion, but can also be a mono-, divalent cation, and B may be 3d, 4d or 5d transition elements having an appropriate oxidation state required for charge balance to give rise to the composition, $A_2B_2O_7$. This structure is closely related to fluorite and can be considered as an ordered, defective fluorite structured materials with anion vacancies (Erickson *et al* 2002; Stanek *et al* 2002). Owing to their unique structural characteristics, pyrochlore oxides show high chemical stability, high catalytic activity, high melting temperature, relatively low conduction temperature and excellent ion conductivity. Yttrium titanate ($Y_2Ti_2O_7$), one of the typical pyrochlore compounds, recently has received considerable attention as a possible candidate for application as oxygen–ion conductor (Shlyakhtina *et al* 2008; Wuensch *et al* 2000), alternative materials to immobilize nuclear solid waste (in particular, actinides) (Ewing *et al* 2004; Pace *et al* 2005), photocatalyst for water-splitting to produce hydrogen

(Higashi *et al* 2005; Abe *et al* 2006), host materials for efficient Er^{3+} luminescence (Jenouvrier *et al* 2005; Ting *et al* 2010), ceramic pigment (Ishida *et al* 1993; Pailh *et al* 2009) and hydrogen storage material (Zhang *et al* 2009).

Usually, yttrium titanate has been prepared by traditional solid state reaction (SSR), i.e. by heat treatment of a stoichiometric mixture of yttria and titania at high temperature for long reaction time (1300°C for 40 h or 1500°C for several h) (Ault and Welch 1966). And also, repeated cycles of grinding and firing of starting oxide components are required to complete the solid state reaction. In spite of this, high pure, composition-homogenous, and nanoscale products are difficult to obtain. Compared with bulk materials, nano-structured ones exhibit outstanding physio-chemical properties; it, therefore, is of great significance to develop alternative synthesis route for pyrochlore $A_2B_2O_7$ nanoparticles at relatively low temperature. Recently, several soft-chemistry methodologies, such as coprecipitation (Hector and Wiggin 2004) and sol–gel method (Lin *et al* 2007), and hydrothermal approach (Li *et al* 2006b; Tang *et al* 2009), have been attempted to prepare nanoscale pyrochlore oxides under relative mild conditions. One of the widely used sol–gel methods, the Pechini approach, developed by Pechini in 1967, is based on a polymeric precursor, in which metal ions are uniformly distributed. During the calcination step the polymeric network collapses and the metal oxide powder is left. The powders

* Author for correspondence (weiping_gong@mail.csu.edu.cn)

are extremely pure and highly homogeneous compared to powders prepared with conventional methods. The aim of this contribution is to exploit citric acid as chelator to prepare high-pure pyrochlore-type $Y_2Ti_2O_7$ nanoparticles at lower reaction temperature.

2. Experimental

2.1 Synthesis of yttrium titanate nanoparticles

Yttrium titanate nanoparticles were synthesized by the citric acid sol-gel route using tetrabutyl titanate and yttria as starting materials. Anhydrous citric acid (CA, $C_6H_8O_7$, A.R.) and absolute ethanol (C_2H_5OH , A.R.) were used as chelator and solvent, respectively. Tetrabutyl titanate [$Ti(OBu)_4$, A.R.] and yttria (Y_2O_3 , 99.99%) were used as the precursors of Ti and Y, respectively. The molar rate of Ti/Y was determined at 1/1, and the amount of citric acid was controlled at $n_{CA}/(n_Y + n_{Ti}) = 2.5$. First a given amount of Y_2O_3 was dispersed in a spot of water and then concentrated HNO_3 was added to it dropwise to dissolve the rare-earth oxide under magnetic stirring, and the excessive HNO_3 was removed completely by slow heating. Subsequently, an appropriate amount of citric acid was dissolved thoroughly in absolute ethanol, and the stoichiometric ratio, $Ti(OBu)_4$, was added drop by drop and the mixture was stirred vigorously until it became homogeneous transparent solution. The solution was poured into the upper solution. The mixture solution was placed in an $80^\circ C$ water bath to vapourize water and excessive solvent, then became highly viscous, and, finally, changed into transparent glassy gel. Noteworthy is that no visible formation of precipitation or turbidity was observed during chelation or gelation. Xerogel is called dried precursor of $Y_2Ti_2O_7$, which was heat-treated at desired temperatures (700 – $900^\circ C$) in static air on an Al_2O_3 boat with a heating rate of $5^\circ C/min$ and dwelling time of 1 h, followed by furnace cooling to room temperature naturally. For comparison, yttrium titanate was also prepared from stoichiometric mixture of yttria and titania by traditional solid state reaction (SSR) according to Ault and Welch (1966).

2.2 Characterization of yttrium titanate nanoparticles

FT-IR spectra (FT-IR Avatar 380, Thermo Nicolet Corporation, USA) was utilized to monitor the structural changes of compounds with a scan range of 4000 – 400 cm^{-1} during the preparative process. Thermogravimetry (TG) and differential thermal analysis (DTA) (TG/DTA851, MAC Science Company, Tokyo, Japan) were operated with the calefactive velocity of $10^\circ C/min$ in air atmosphere to follow the physicochemical changes of xerogel during calcination. The crystalline phase structure of products was determined by X-ray diffraction analysis (XRD; Rigaku D/max-2000) using CuK_α radiation, $\lambda = 0.154056\text{ nm}$, $40\text{ kV}/300\text{ mA}$, scan rate of $2\theta\ 4^\circ/min$, scan range of (2θ)

10 – 80°). Nanocrystallite sizes were estimated from XRD spectra by use of Scherrer's equation:

$$D = (k\lambda)/(\beta\cos\theta),$$

where D is the grain size, k a constant (shape factor), λ the X-ray wavelength, β the full-width-at-half-maximum (FWHM) of a characteristic diffraction peak and θ the diffraction angle. The microstructures and average size of samples were examined by transmission electron microscopy (TEM, JEOL-2010F/2200Fs, Japan) with an accelerating voltage of 200 kV, while the atomic composition was determined using an EDX spectrometer attached to the FESEM (FESEM, JSM-7001F, JEOL Japan). TEM samples were prepared by dispersing the powder in absolute alcohol by ultrasonic treatment, dropping onto a porous carbon film supported on a copper grid, and then dried in air. The Brunauer-Emmett-Teller (BET) surface area was evaluated by the amount of nitrogen adsorption at 77 K in a constant volume adsorption apparatus (Coulter SA 3100).

3. Results and discussion

3.1 FT-IR spectra

FT-IR spectra were used to monitor the structural changes of compounds during the process to investigate the reaction and uniform distribution mechanism of reactants during the preparative process. It can be seen that strong coordination interaction existed between metal precursors and citric acid. The bands around 3435 cm^{-1} and 1636.8 cm^{-1} are attributed to the stretching vibration of hydroxyl group, OH (Li *et al* 2006a), for which moisture present in the samples can be accounted. The absorption peaks around 1385 cm^{-1} are assigned to the symmetric vibration mode of carbonyl groups due to the adsorption of CO_2 molecule in the samples. Comparing figure 1(a) to figure 2(b), the band around 1730.3 cm^{-1} , which is the stretching vibration of $C=O$ in $-COOH$, disappeared in the products calcined at $750^\circ C$. Two bands at 1398.8 and 1204 cm^{-1} was observed in the xerogel, which are ascribed to the $COO-$ stretching vibration for Ti^{4+} - carboxylic acid complex (Xiong *et al* 1997) and Y^{3+} - carboxylic acid complex (Akcora *et al* 2005), respectively, suggesting that there existed strong coordination interaction between Ti^{4+} , Y^{3+} and citric acid. Both the bands disappeared when the precursor was calcined at $750^\circ C$. In addition, two bands at 560.5 cm^{-1} and 460.2 cm^{-1} were observed in precursor gel, which was assigned to the stretching vibration of $Ti-O$ and $Y-O'$, respectively (Coutier *et al* 2001). In $Y_2Ti_2O_7$ powder, however, the bands at 568.2 cm^{-1} , 468.3 cm^{-1} and 410 cm^{-1} are ascribable to $Ti-O$, $Y-O'$ and $Y-O$ stretching vibration, respectively which are the main features of the titanate pyrochlore spectra (Subramanian *et al* 1983). The slight difference of the absorption position of $Ti-O$ and $Y-O'$ in precursor and $Y_2Ti_2O_7$ powder, can be explained as the different chemical environment. Owing to

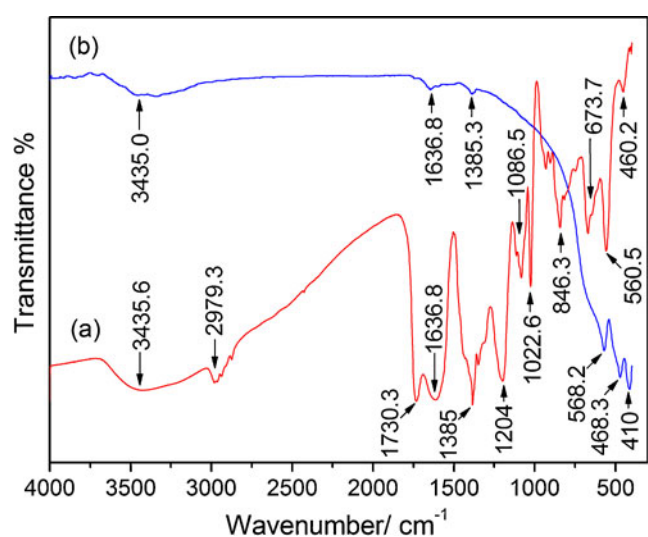


Figure 1. FT-IR spectra of (a) $Y_2Ti_2O_7$ xerogel and (b) $Y_2Ti_2O_7$ calcined at $750^\circ C$.

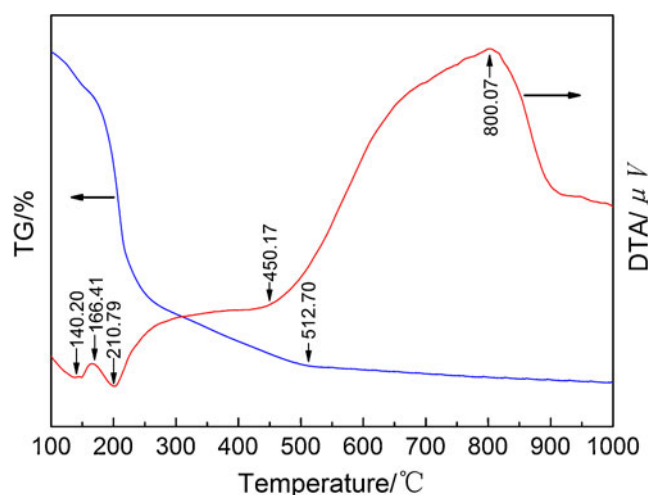


Figure 2. TG-DTA curve of $Y_2Ti_2O_7$ xerogel in the temperature range $100\text{--}1000^\circ C$.

the strong interaction between metal ions and citric acid, Ti^{4+} and Y^{3+} were uniformly and highly dispersed in citric acid, achieving molecular level distribution, which may help to dramatically lower the calcining temperature and make sure that the as-obtained products are ultrafine and ultrapure. This supposition was fully confirmed by XRD results below.

3.2 TG-DTA

TG-DTA experiment was utilized in order to determine the decomposition of precursor and the transformation of $Y_2Ti_2O_7$ crystal phase. The TG curve shows a continuous weight loss up to about $512^\circ C$, the weight loss is due to

dehydration and decomposition of the organics. As seen in the DTA curve, the first endothermic peak ($140\text{--}20^\circ C$) is assigned to the volatilization and desorption of water and ethanol. The second endothermic peak ($210\text{--}79^\circ C$) is caused by the evaporation and burning of organic substances. A large exothermic range ($250\text{--}450^\circ C$) is observed, which is attributed to the combustion of citric acid complex. The broad and strong exothermic peak ($800^\circ C$) is related to the crystal lattice energy by the formation of pyrochlore oxide phase and its complete crystallization. No further weight loss was found up to $900^\circ C$, indicating that the $Y_2Ti_2O_7$ crystals can be prepared at lower temperature by citric acid sol-gel method. The results are in good agreement with XRD experiments.

3.3 XRD

Figure 3 shows the XRD patterns of the $Y_2Ti_2O_7$ powders by CAM calcined in static air at various temperatures ($700\text{--}900^\circ C$) for 1 h. It is obvious that the precursor heat-treated at $700^\circ C$ for 1 h is primarily amorphous as shown by the broad continuum in XRD pattern in figure 3(a). Dramatic crystallization has occurred during the calcination of precursor at $750^\circ C$ for 1 h. And all of the XRD reflections of precursor that has been heat-treated at temperature above $750^\circ C$ exhibit single phase $Y_2Ti_2O_7$ with a pyrochlore structure, the XRD pattern of which is indexed based on face-centred cubic lattice ($a = 10.089 \text{ \AA}$) as reported previously (JCPDS No. 89-2065) (Brixner 1964). Additionally, with the increase of calcination temperature, the intensity of each peak grew and the position of 2θ indicating a pyrochlore structure did not change, which means that during the calcination step, no other impure phases such as Y_2O_3 and TiO_2 were formed.

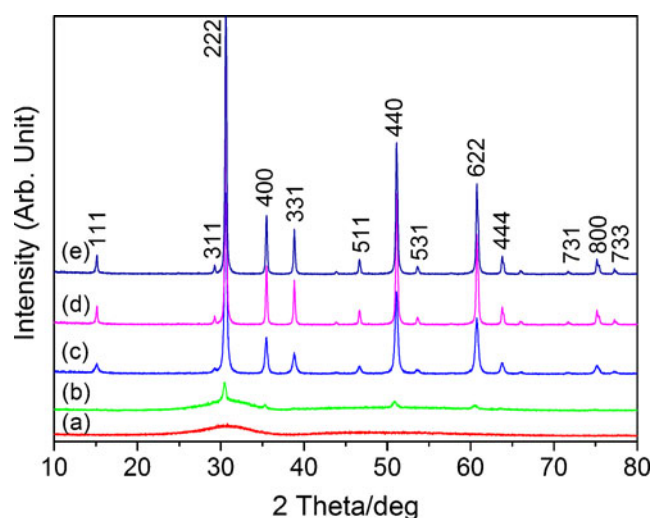


Figure 3. XRD patterns of $Y_2Ti_2O_7$ calcined at different temperatures by citric acid (a) $700^\circ C$, (b) $725^\circ C$, (c) $750^\circ C$, (d) $800^\circ C$ and (e) $900^\circ C$.

Therefore, before the calcination step, the two components (Y and Ti) in the xerogel were almost homogeneous. And also, based on the Scherrer equation, the average grain size of $Y_2Ti_2O_7$ obtained from a calcining temperature of $750^\circ C$ was about 25 nm (the value is calculated by FWHM of the most intense line at the diffraction angle 2θ 30.58 which is 0.342), which is fully confirmed by TEM results below.

For the solid-state reaction route (see figure 4), however, no $Y_2Ti_2O_7$ phase was observed in the product when calcinated at $750^\circ C$, only the phase of anatase-type TiO_2 and Y_2O_3 were detected. When the sample was heated at $1100^\circ C$, the pyrochlore structure was identified, and also there existed still the phase of unreacted rutile-type TiO_2 and Y_2O_3 . Only when the temperature was raised to $1500^\circ C$ and the calcination time was extended to 10 h, a pure phase of $Y_2Ti_2O_7$ was completely formed. These results indicate that the pyrochlore oxide $Y_2Ti_2O_7$, which usually forms at high temperature in conventional method ($1500^\circ C$) with a long reaction time (10 h) (Ault and Welch 1966), can be successfully synthesized at a relatively low temperature ($750^\circ C$) with shortened reaction time (1 h) by the modified sol-gel method. This technique is beneficial to energy-saving and environment pollution; and it is a cheap and green approach to achieve excellent pyrochlore oxides.

3.4 TEM and EDX spectra

Transmission electron microscopy (TEM) was employed to obtain direct information about the size and structure of the prepared $Y_2Ti_2O_7$ nanocrystals. The TEM results of $Y_2Ti_2O_7$ prepared from a calcining temperature of $750^\circ C$ with dwelling time of 1 h are shown in figure 5. From figure 5(a), it can be found that quasi-spherical $Y_2Ti_2O_7$ nanoparticles have good dispersibility, and the average size

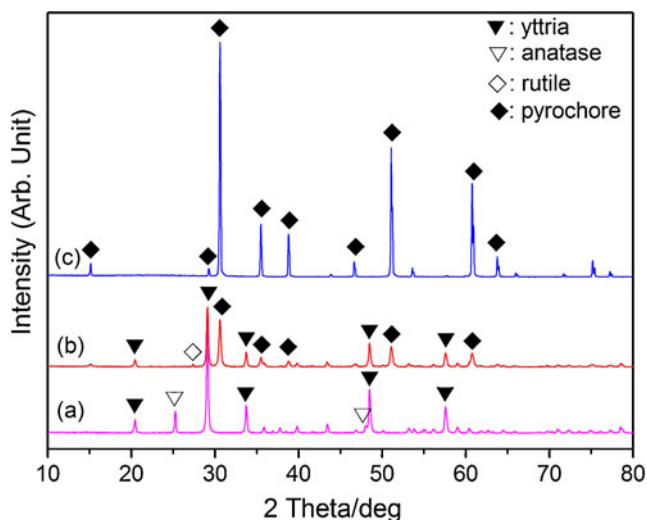


Figure 4. XRD patterns of $Y_2Ti_2O_7$ calcined at different temperatures by solid-state reaction: (a) $750^\circ C$, (b) $1100^\circ C$, (c) $1500^\circ C$.

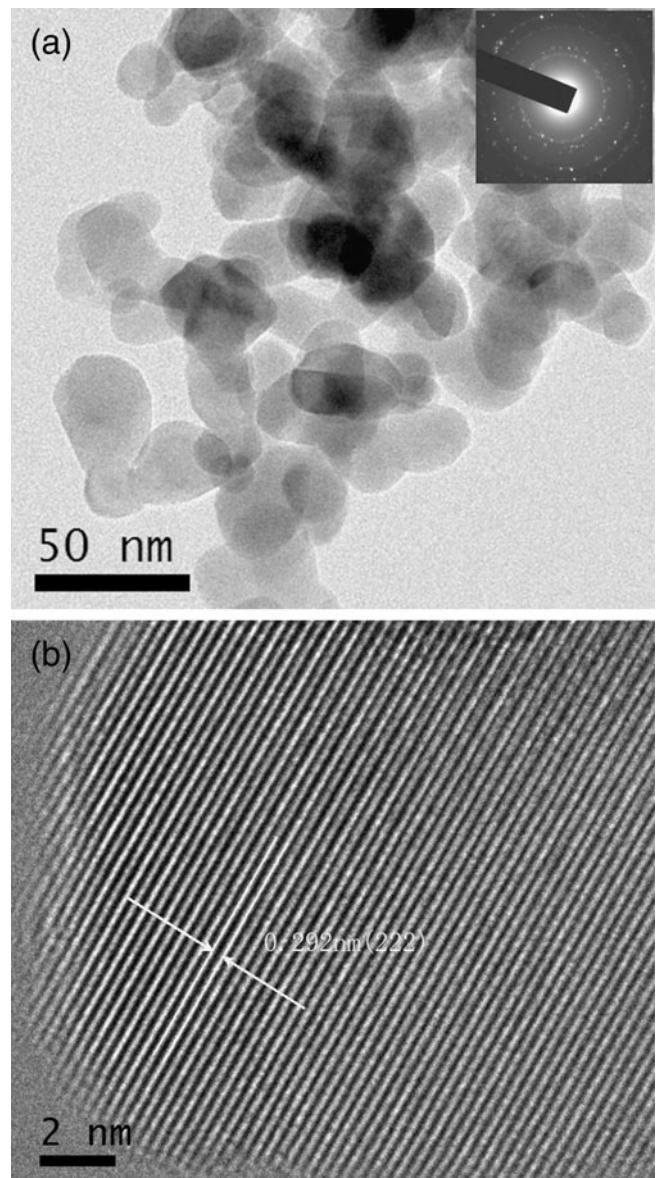


Figure 5. TEM micrographs of $Y_2Ti_2O_7$ calcined at $750^\circ C$ for 1 h by modified sol-gel method: (a) TEM, (b) HRTEM. The inset in (a) shows the corresponding electron diffraction patterns.

estimated from TEM is around 20–30 nm, which is quite consistent with XRD results. The inset in figure 5(a) shows the corresponding electron diffraction patterns, which is the characteristic rings of nano-polycrystals. In figure 5(b), typical high-resolution transmission electron microscopy (HRTEM) images indicate clear and regular crystal lattice distance suggesting that highly crystalline $Y_2Ti_2O_7$ were formed. The lattice fringes with an interplanar distance of 0.292 nm obtained from the HRTEM images was attributed to the (222) plane of the cubic structure. According to the EDX analysis, it can be seen that there is no other element than Y, Ti and O on the product surface (figure 7), and the atomic ratio of Y:Ti:O is 18.15:18.20:63.65 (see the inset

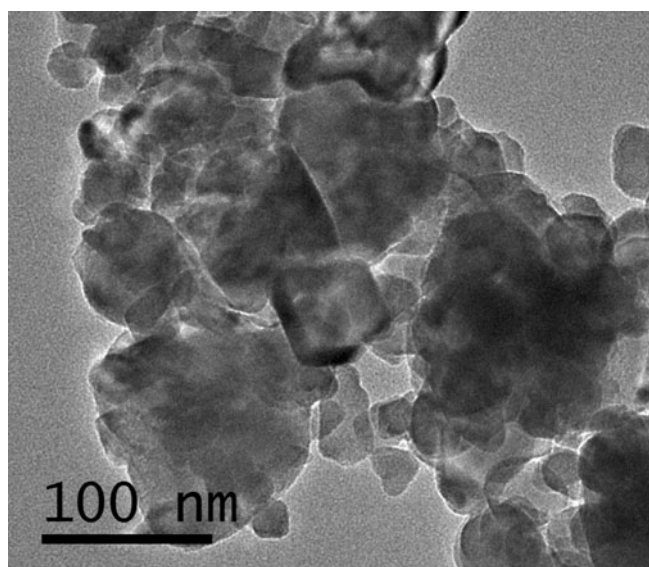


Figure 6. TEM image of $Y_2Ti_2O_7$ calcined at $1500^\circ C$ for 8 h via solid state reaction route.

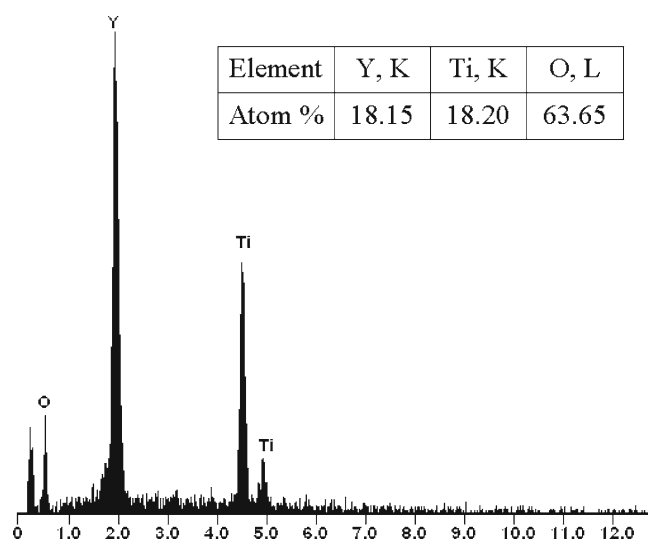


Figure 7. EDX spectrum of $Y_2Ti_2O_7$ calcined at $750^\circ C$ for 1 h by modified sol-gel method.

in figure 7), suggesting that the $n_Y:n_{Ti}:n_O$ is 2:2:7, which is uniform to the theoretical composition.

For comparison, the morphology and dispersibility of $Y_2Ti_2O_7$ fabricated by solid-state reaction were also presented (see figure 6). The morphology and dispersibility were quite different from those of modified sol-gel method. It was very difficult to identify the morphology of $Y_2Ti_2O_7$ and its dispersibility was quite low. So the catalytic activity of $Y_2Ti_2O_7$ may be restricted by these two aspects. And also, the BET surface area of $Y_2Ti_2O_7$ calculated from N_2 isotherms at 77 K was about $50 \text{ m}^2/\text{g}$, and is quite larger than those of traditional solid-state reaction products ($5 \text{ m}^2/\text{g}$) and

other soft-chemistry routes (Rao *et al* 2007). These excellent physical properties of the samples obtained by citric acid method, such as more regular morphology, higher dispersibility, and larger BET surface area may result in better behaviour in hydrogen storage and photocatalytic reaction.

4. Conclusions

Pyrochlore-type yttrium titanate nanoparticles were prepared by citric acid sol-gel process at $750^\circ C$ for 1 h. The obtained $Y_2Ti_2O_7$ is nearly sphere-like and exhibits good crystallinity, smaller average size (20–30 nm) and larger BET surface area ($50 \text{ m}^2/\text{g}$). This research provides a simple soft-chemistry route to synthesize nanoscale pyrochlore-oxide $Y_2Ti_2O_7$ at lower temperatures and with shortened reaction time. This approach can also be applied for the preparation of other pyrochlore oxides nanoparticles.

Acknowledgements

The funding for projects came from the Natural Science Foundation of China (No. 50634060), the Science Centre of Phase Diagrams & Materials Design and Manufacture and Natural Science, Foundation of Jiangxi Province (No. 2009GZH0002 and No. 2009GZH0004). The support from the Special Talents of Higher Education Office of Guangdong Province is greatly appreciated.

References

- Abe R, Higashi M, Sayama K, Abe Y and Sugihara H 2006 *J. Phys. Chem.* **B110** 2219
- Akcora P, Zhang X, Varughese B, Briber R M and Kofinas P 2005 *Polymer* **46** 5194
- Ault J and Welch A 1966 *Acta Crystallogr.* **20** 410
- Brixner L 1964 *Inorg. Chem.* **3** 1065
- Coutier C, Meffre W, Jenouvrier P, Fick J, Audier M, Rimet R, Jacquier B and Langlet M 2001 *Thin Solid Films* **392** 40
- Erickson E E, Gray D, Taylor K, Macaluso R T, LeTard L A, Lee G S and Chan J Y 2002 *Mater. Res. Bull.* **37** 2077
- Ewing R C, Weber W J and Lian J 2004 *J. Appl. Phys.* **95** 5949
- Hector A L and Wiggin S B 2004 *J. Solid State Chem.* **177** 139
- Higashi M, Abe R, Sayama K, Sugihara H and Abe Y 2005 *Chem. Lett.* **34** 1122
- Ishida S, Ren F and Takeuchi N 1993 *J. Am. Ceram. Soc.* **76** 2644
- Jenouvrier P, Boccardi G, Fick J, Jurdyc A M and Langlet M 2005 *J. Lumin.* **113** 291
- Li G Z, Yu M, Wang R S, Wang Z L, Quan Z W and Lin J 2006a *J. Mater. Res.* **21** 2232
- Li K W, Wang H and Yan H 2006b *J. Mol. Catal. A: Chem.* **249** 65
- Lin K M, Lin C C, Hsiao C Y and Li Y Y 2007 *J. Lumin.* **127** 561
- Pace S, Cannillo V, Wu J, Boccaccini D N, Seglem S and Boccaccini A R 2005 *J. Nucl. Mater.* **341** 12
- Pailh N, Gaudon M and Demourgues A 2009 *Mater. Res. Bull.* **44** 1771
- Pechini M 1967 US Patent 3 330 697

- Rao K K, Anantharamulu N, Salagram M and Vithal M 2007 *Spectrochim. Acta Part A* **66** 646
- Shlyakhtina A V, Savvin S N, Levchenko A V, Boguslavskii M V and Shcherbakova L G 2008 *Solid State Ionics* **179** 985
- Stanek C R, Minervini L and Grimes R W 2002 *J. Am. Ceram. Soc.* **85** 2792
- Subramanian M A, Aravamudan G and Subba Rao G V 1983 *Prog. Solid State Chem.* **15** 55
- Tang Z, Zhou L, Yang L and Wang F 2009 *J. Alloys Compd* **481** 704
- Ting C C, Chang C W, Chuang L C, Li C H and Chiu Y S 2010 *Thin Solid Films* **518** 5704
- Wuensch B J et al 2000 *Solid State Ionics* **129** 111
- Xiong G, Zhi Z L, Yang X J, Lu L D and Wang X 1997 *J. Mater. Sci. Lett.* **16** 1064
- Zhang L, Zhang W, Zhu J, Hao Q, Xu C, Yang X, Lu L and Wang X 2009 *J. Alloys Compd* **480** L45